

Anomalous diffusion and elastic mean free path in disorder-free multi-walled carbon nanotubes

Shidong Wang and Milena Grifoni
Theoretische Physik, Universität Regensburg, 93040 Germany

Stephan Roche
CEA/DSM/DRFMC/SPSMS/GT, 17 avenue des Martyrs, 38054 Grenoble, France
 (Dated: June 15, 2021)

We explore the nature of anomalous diffusion of wave packets in disorder-free incommensurate multi-walled carbon nanotubes. The spectrum-averaged diffusion exponent is obtained by calculating the multifractal dimension of the energy spectrum. Depending on the shell chirality, the exponent is found to lie within the range $1/2 \leq \eta < 1$. For large unit cell mismatch between incommensurate shells, η approaches the value $1/2$ for diffusive motion. The energy-dependent quantum spreading reveals a complex density-of-states-dependent pattern with ballistic, super-diffusive or diffusive character.

PACS numbers: 73.63.Fg, 73.23.-b, 72.10.Di

The understanding of charge transport in structurally clean systems, with complex and aperiodic long-range correlations, has been the subject of intense debate during the past two decades [1]. The quantum dynamics in most of these systems has been described as an anomalous quantum diffusion process, related to the multifractal nature of the electronic states and spectra [2]. These unconventional transport mechanisms are incompatible with a dominant transport length scale such as the elastic mean free path, and the occurrence of a diffusive regime. Recently, the discovery of carbon nanotubes has provided a whole class of new quasi-one-dimensional systems with spectacular effects of topological arrangements of carbon atoms on the electronic spectra [3, 4]. The multi-walled nanotubes (MWNTs) are intrinsic incommensurate objects since, due to registry mismatch between neighboring shells, there are very few cases in which the respective symmetries of individual shells allow finding a common unit cell for the whole object. In most cases, the unit cell length (along the nanotube axis) ratio between adjacent shells is an irrational number, and the MWNT taken as a whole becomes an incommensurate object [3]. In recent years, mechanical [5] and electronic [6, 7, 8, 9, 10, 11, 12] properties of double- and triple-walled incommensurate nanotubes (i-DWNTs and i-TWNTs, respectively) have been intensively investigated. Roche *et al.* [6] first reported on anomalous diffusion properties of i-DWNTs and i-TWNTs by numerical analysis of the wave-packet propagation. Signatures of anomalous diffusion were further inferred by the evaluation of the energy spacing distribution of energy levels [7], exhibiting Wigner-Dyson, Poisson and semi-Poissonian statistics depending on the position of the Fermi level. In a recent work [11], the existence of a finite (energy-dependent) elastic scattering rate for electrons in the outer shell of a disorder-free i-DWNTs was analytically shown to be a consequence of helicity-determined selection rules for inter-shell tunnel-

ing [8, 12].

Aim of this letter, is to establish the connection between spectral and clarify the dynamical properties of i-DWNTs, i-TWNTs and in general MWNTs. Our results provide a deeper insight on why, experimentally, MWNTs typically, but not always [13, 14] exhibit normal diffusion behavior, with an energy dependent mean free path [15]. However, we predict global anomalous diffusive behavior in i-DWNTs and in many i-TWNT systems. To this extend, first we calculate the *spectrum-averaged* diffusion exponent η , which describes the spread in time of an initially localized wave packet by looking at the mean square displacement

$$\overline{X^2}(t) \simeq t^{2\eta} . \quad (1)$$

For this we evaluate the multifractal dimension $1/2 \leq D_{-1} < 1$ of the energy spectrum of various incommensurate, tunnel coupled, i-DWNTs and i-TWNTs, and use the relation $\eta = D_{-1}$ [16, 17]. We find a good agreement with previous calculations using a wave-packet propagation approach [6, 9]. We find that the exponent η strongly depends on the chirality and on the number of shells. In particular, for fixed number of shells, e.g. two, one can find that η is closer to the value $1/2$, characteristic of normal diffusion, if at least one shell has a large unit cell. Also upon increasing the number of shells the diffusive limit $1/2$ is more rapidly approached. For example, for the i-TWNT (6, 4)@(17, 0)@(15, 15) is already $\eta \simeq 1/2$ such that for such a tube some elastic mean free path can be extracted from the wave-packet evolution. In contrast, for the (5, 5)@(17, 0)@(15, 15) i-TWNT, with a very small unit cell of the (5,5) shell, the diffusion remains anomalous, and thus no *global* mean free path can be extracted. While the exponent η describes spectrum-averaged properties, more information about the interplay between density of states and degree of anomaly can be extracted from the energy dependent quantities.

Thus wave-packet spreading is investigated by solving the time-dependent Schrödinger equation and calculating the *energy-dependent* quantum spreading

$$\ell(E, t) = \frac{X^2(E, t)}{v(E)t} = \frac{\text{Tr}\{\delta(E - \hat{\mathcal{H}})(\hat{\mathcal{X}}(t) - \hat{\mathcal{X}}(0))^2\}}{\text{Tr}\{\delta(E - \hat{\mathcal{H}})\}v(E)t}.$$

Here $\delta(E - \hat{\mathcal{H}})$ is the spectral measure operator, whose trace gives the total density of states $n(E)$, $\hat{\mathcal{H}}$ is the system's Hamiltonian, and $\hat{\mathcal{X}}(t)$ is the position operator along the tube axis. Finally, $v(E)$ is the group velocity at energy E . In some situations $\ell(E, t)$ becomes time-independent such that energy-dependent elastic mean free paths can be defined even if the global exponent η is not $1/2$!

Our starting model to evaluate wave-packet spreading is the tight-binding Hamiltonian for a MWNT with M shells, where only one p_{\perp} -orbital per carbon atom is kept, and with zero on-site energies. With a nearest-neighbor hopping γ_0 on each layer n , and hopping β between neighboring layers, it has the form [18]:

$$\begin{aligned} \hat{\mathcal{H}} = & \gamma_0 \sum_{n=1}^M \sum_{\langle i, j \rangle} |p_{\perp}^{n, j}\rangle \langle p_{\perp}^{n, i}| \\ & - \beta \sum_{\langle n, m \rangle} \sum_{i, j} \cos(\theta_{ij}) e^{-\frac{d_{ij}-a}{\delta}} |p_{\perp}^{j, n}\rangle \langle p_{\perp}^{i, m}|, \end{aligned} \quad (2)$$

where $\langle n, m \rangle$ and $\langle i, j \rangle$ are sums over nearest shells and nearest neighboring atoms, respectively. Moreover, θ_{ij} is the angle between the p_{\perp}^i and p_{\perp}^j orbitals, and d_{ij} denotes their relative distance. The parameters used here are: $\gamma_0 = 2.9$ eV, $a = 3.34$ Å, $\delta = 0.45$ Å [3]. An ab-initio estimate gives for the intershell coupling $\beta \simeq \gamma_0/8$ [18]. Starting from Eq. (2), the spreading of wave packets is now evaluated along two different routes. For our first approach, we start by observing that the dynamics of wave packets in a system is strongly related to the properties of the system's energy spectrum. The latter can be generally divided into absolutely continuous, singular continuous and pure point parts [19]. The wave packets spread ballistically if the energy spectrum is absolute continuous and are localized in systems with purely point-like spectra. If the spectrum is singular continuous the wave packets anomalously spread [20, 21, 22]. The singular continuous spectrum is a multifractal object which can be characterized by a set of fractal dimensions D_q [23]. Piéchon has shown that, at large times $t \rightarrow \infty$, the moments spread as $\overline{X^q}(t) \sim t^{qD_{1-q}}$, with D_q the fractal dimension of the energy spectrum [16]. Then, the spreading of a wave packet is determined by D_{-1} . The motion of wave packets in a system with singular continuous energy spectrum will be normal diffusive if $D_{-1} = 1/2$, or anomalous diffusive if $1/2 < D_{-1} < 1$. The energy spectrum of an incommensurate system is usually singular continuous, or maintain intrinsic self-similar features [2].

Therefore, one may expect some anomalous diffusive behavior of wave packets in i-DWNTs. In order to calculate the energy spectrum of an i-DWNT, we approximate the irrational ratio of the unit cell lengths of the inner and outer shells by one of its convergents, which is the rational number obtained by truncating the continued fraction representation of the given irrational number up to a certain term [2, 24]. That is, we approximate the i-DWNT by a commensurate DWNT. As the chosen convergent becomes closer to the irrational unit cell ratio, the energy spectrum of the commensurate DWNT gets closer to that of the i-DWNT under study. We calculate the energy spectrum of the commensurate DWNT by direct diagonalization of the Hamiltonian in Eq.(2). After computing the energy spectrum, we count the numbers of boxes $N(l)$ with length $l = \Delta E/2^n$ needed to cover it. Here ΔE is the range of the energy spectrum and n is a positive integer. Thus, the probability density $p_i(l)$ is obtained for each box by calculating the ratio of the number of points falling into the box $\Lambda_i(l)$ to the total number of points in the data. The set of fractal dimensions D_q can be defined as

$$\sum_{i=1}^{N(l)} p_i^{q+1}(l) \sim l^{qD_{q+1}}, \quad \text{as } l \rightarrow 0.$$

For a simple fractal object, that is, the probability density $p_i(l)$ is the same for each box $\Lambda_i(l)$, all general dimensions defined above have the same values D_F . In this case, the probability density is $p_i(l) = 1/N(l)$, with $N(l) \sim l^{-D_F}$. Therefore is $D_{q+1} = D_F$ for any q . Here, D_F is the fractal (box-counting) dimension. In general, the distribution of points in a fractal object is different for different boxes. That is, the probabilities of finding a point in the different boxes are different. If $q = -1$, one has $D_0 = D_F$. For $q = -2$ the dimension D_{-1} can be calculated by

$$D_{-1} = -\frac{1}{2} \lim_{l \rightarrow 0} \frac{\ln \sum_{i=1}^{N(l)} p_i^{-1}(l)}{\ln l}. \quad (3)$$

Hence, the dimension D_{-1} is extracted from a linear regression fit to the plot of $\mathcal{A}_l \equiv -\frac{1}{2} \ln \sum_{i=1}^{N(l)} p_i^{-1}(l)$ as a function of $\ln l$. As an example, Fig. 1 shows results for the energy spectrum of the i-DWNT (9, 0)@(10, 10). As discussed in Ref. [11], the incommensurability of the two unit cells yields a non-vanishing intershell tunneling only when helicity-determined selection rules are fulfilled, which can occur only if enough sub-bands in each shell become populated. In turn, this yields a finite lifetime for electrons in one shell due to effective back-scattering processes. Here we show that these features are also reflected in the energy spectrum which, as shown in Fig. 1, exhibits a fractal character. We find that within the energy range $[-12.664$ eV, 12.898 eV] the fractal dimension converges to the value $\eta = 0.88$, when the incommensurate ratio $T_{(10,10)}/T_{(9,0)} = 1/\sqrt{3}$ is approxi-

ated by the 6th convergent $15/26$ obtained by truncating the continued fraction expression of $1/\sqrt{3}$. This value is the same as found from numerical wave-packet propagation of initially localized wave packets [6]. Here, $T_{(n,m)} = a_0\sqrt{3(n^2 + nm + m^2)}/\text{GCD}$ is the length of the axial unit cell of shell (n, m) , with the carbon-carbon bond length a_0 and GCD being the greatest common divisor of $(2n + m)$ and $(m + 2n)$.

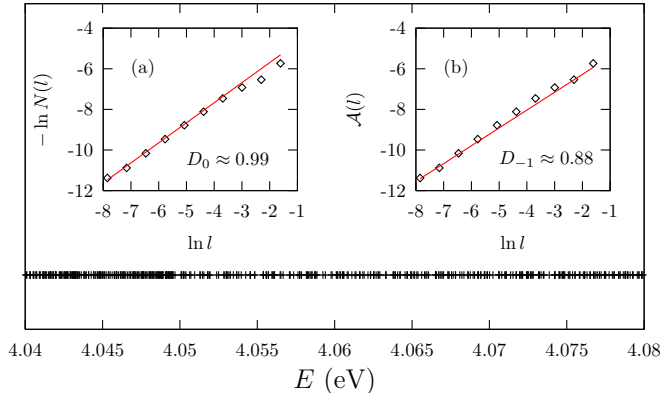


FIG. 1: (Color online) Fractal character of the energy spectrum of the i-DWNT $(9,0)@(10,10)$ in the range $[4.04 \text{ eV}, 4.08 \text{ eV}]$. Inset (a): Plot of $-\ln N(l)$ vs. $\ln l$ as determined from the energy spectrum. A linear fit to the data corresponding to the shortest lengths l yields the fractal dimension D_0 . Inset (b): Plot of $\mathcal{A}_l = -\frac{1}{2} \ln \sum_{i=1}^{N(l)} p_i^{-1}(l)$ vs. $\ln l$ as determined from the energy spectrum. The slope is the fractal dimension D_{-1} .

In order to understand the role of chirality, we have also investigated the cases of the $(6,4)@(17,0)$ and $(5,5)@(17,0)$ i-DWNTs, differing in the chirality of the inner shell. One has $T_{(17,0)}/T_{(5,5)} = \sqrt{3}$, while $T_{(17,0)}/T_{(6,4)} = 1/\sqrt{19}$. The difference in the two exponents is noticeable: $\eta_{(5,5)@(17,0)} \approx 0.88$ and $\eta_{(6,4)@(17,0)} \approx 0.82$. We attribute the smaller exponent of the $(6,4)@(17,0)$ i-DWNT compared to that of the $(5,5)@(17,0)$ i-DWNT to the larger unit shell mismatch. Having in mind the i-DWNT $(5,5)@(17,0)$, we add an additional outer shell and consider the i-TWNTs $(5,5)@(17,0)@(15,15)$ and $(6,4)@(17,0)@(15,15)$. For the first TWNT the diffusion is still anomalous with $\eta_{(5,5)@(17,0)@(15,15)} \approx 0.88$. However, the effect of the additional armchair shell $(15,15)$ is to *randomize* the energy spectrum of the $(6,4)@(17,0)@(15,15)$. To be definite, already for the approximation $26 : 26 : 15$ to the ratios $3\sqrt{19} : 3 : \sqrt{3}$ we find the value $\eta \approx 0.60$, as shown in Fig. 2. Notice that, since D_{-1} is defined in the limit of box length $l \rightarrow 0$, for the linear fit in Fig. 2 the five points corresponding to the smallest lengths l have been considered.

As second calculation route, the energy-dependent and time-dependent wave-packet spreading $\ell(E, t)$ is analyzed numerically. The resolution of the time-dependent

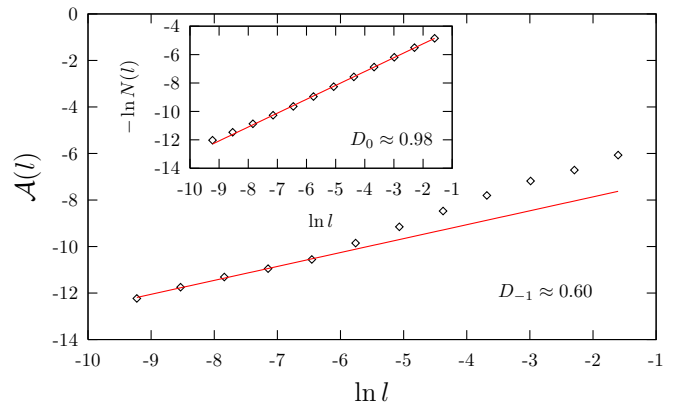


FIG. 2: (Color online) Plot of $\mathcal{A}_l = -\frac{1}{2} \ln \sum_{i=1}^{N(l)} p_i^{-1}(l)$ vs. $\ln l$ as extracted from the energy spectrum of the $(6,4)@(17,0)@(15,15)$ i-TWNT. The linear fit to the data corresponding to the shortest box lengths l yield the fractal dimension D_{-1} . Inset: Plot of $-\ln N(l)$ vs. $\ln l$ for the same i-TWNT. The slope is the fractal dimension D_0 .

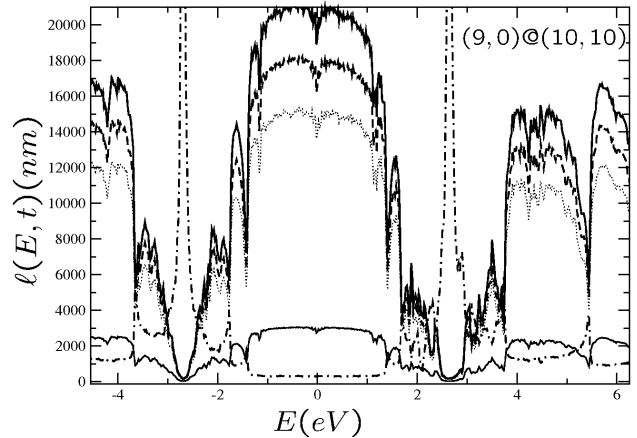


FIG. 3: (Color online) Energy-dependent behavior of the spreading $\ell(E, t)$ for the $(9,0)@(10,10)$ i-DWNT, at several times t (solid line $t = 1000T$, dotted $t = 5000T$, dashed $t = 6000T$, bold $t = 7000T$, with $T = 14\hbar/\gamma_0$). The rescaled total density of states is also shown (dash-dotted-line).

Schrödinger equation is made by expanding the evolution operator $e^{-i\hat{H}t}$ on a basis of orthogonal polynomials. This method has been demonstrated to provide an efficient real-space computational framework for an order N algorithm [25]. The total length of the MWNTs is finite but several tens of μm -long in order to limit boundary effects. For example, the calculations shown in Figs. 3 and 4 are performed with a finite length of about $24 \mu\text{m}$, whereas the unit time step is taken as $T = 14\hbar/\gamma_0 \simeq 3.18 \text{ fs}$. Most generally, the anomalous quantum spreading is driven by a time dependent power law, $\ell(E, t) = t^{2\eta(E)-1}/v(E)$, whose asymptotic regime gives the conduction regime. When $\ell(E, t)$ tends to some

finite constant at large times, some energy-local elastic mean free path $\ell_{\text{el}}(E)$ can be extrapolated as $\ell_{\text{el}}(E) = \lim_{t \rightarrow \infty} \ell(E, t)$. In Fig. 3 and Fig. 4(main frame), the energy-dependent length scale $\ell(E, t)$ is shown at several chosen elapsed times t , starting from wave packets that are homogeneously spread in real space with random phase on each lattice point.

For the case of $(9, 0)@(10, 10)$ (Fig. 3), and energies in the charge neutrality point vicinity, a careful analysis of propagation over several tens of microns reveals no deviation from a ballistic-like regime with $\eta(E) = 1$. Conversely for a small energy window in a high density of states region, a very slowly varying length is observed. Here the effect of incommensurability becomes more pronounced due to the enlarged electronic population available for scattering. The result of the energy-averaged diffusion exponent gives the global exponent $\eta = 0.88$ intermediate between the value 1 and $1/2$, and in agreement with prior analysis.

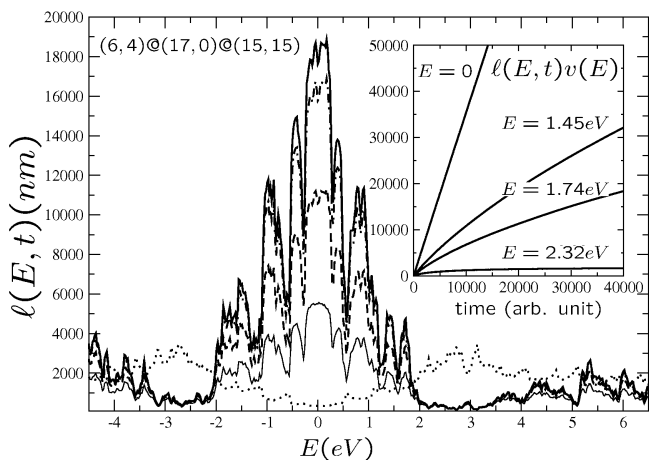


FIG. 4: (Color online) Energy-dependent behavior of $\ell(E, t)$ for the $(6, 4)@(17, 0)@(15, 15)$ i-TWNT, at several times t (solid line $t = 2000T$, dashed $t = 4000T$, dot-dashed $t = 6000T$, bold $t = 6710T$, with $T = 14\hbar/\gamma_0$). The rescaled total density of states is also shown (dotted-line). Inset: time-dependence of the diffusivity $\ell(E, t)v(E)$ at various selected energies.

In the case of stronger incommensurate systems, such as the $(6, 4)@(17, 0)@(15, 15)$ i-TWNT, the tendency towards energy-dependent anomalous conduction becomes even more pronounced. First the region of 2 eV around the charge neutrality point remains almost ballistic, whereas the rest of the electronic spectrum shows a very slower expansion of wave packet in time. The propagation time runs from 0.4 ps ($t = 2000T$) to 1.5 ps ($t = 6710T$), and clearly $\ell(E, t)$ either shows anomalously slow diffusion, or saturates at very short times (inset in Fig. 4). Whenever the saturation limit is clearly reached, a mean free path $\ell_{\text{el}}(E)$ for the whole object can be mean-

ingfully extracted. ℓ_{el} is found to be around 200 nm to 400 nm for energies in between 2 eV to 3.5 eV

To conclude, we found that the energy-averaged exponent η depends crucially on chirality and number of coupled shells with global anomalous behavior strongly pronounced in i-DWNT. When looking to energy-dependent properties, we found that even for i-MWNT exhibiting $\eta(E) \sim 1$ (ballistic spreading) close to the charge neutrality point, some elastic mean free path can be defined in regions of larger density of states where $\eta(E) \sim 1/2$.

-
- [1] M. Kohmoto, Phys. Rev. Lett. **51**, 1198 (1983); E. Macia and D. Dominguez-Adame, Phys. Rev. Lett. **79**, 5301 (1997); S. Roche and D. Mayou, Phys. Rev. Lett. **79**, 2518 (1997); X. Wang, U. Grimm and M. Schreiber, Phys. Rev. B **62**, 14020 (2000).
 - [2] J. B. Sokoloff, Phys. Rep. **126**, 189 (1985).
 - [3] R. Saito, G. Dresselhaus, M. S. Dresselhaus and J. Appl. Phys. **73**, 494 (1993).
 - [4] R. Saito, G. Dresselhaus, M. Dresselhaus, *Physical Properties of Carbon nanotubes* (Imperial College Press, London 1998).
 - [5] A. N. Kolmogorov and V. H. Crespi, Phys. Rev. Lett. **85**, 4727 (2000).
 - [6] S. Roche et al., Phys. Rev. B **64**, 121401(R) (2001); *ibidem* Phys. Lett. A **285**, 94 (2001).
 - [7] K.-H. Ahn *et al.*, Phys. Rev. Lett. **90**, 026601 (2003).
 - [8] Y.-G. Yoon *et al.*, Phys. Rev. B **66**, 073407 (2002).
 - [9] F. Triozon *et al.*, Phys. Rev. B **69**, 121410(R) (2004).
 - [10] S. Uryu, Phys. Rev. B **69**, 075402 (2004); J. Chen and L. Yang, J. Phys. Cond. Matt. **17**, 957 (2005); A. Mayer, Carbon **43**, 717 (2005); S. Uryu and T. Ando, Phys. Rev. B **72**, 245403 (2005).
 - [11] S. Wang and M. Grifoni, Phys. Rev. Lett. **95**, 266802 (2005).
 - [12] A.M. Lunde, K. Flensberg and A.-P. Jauho, Phys. Rev. B **71**, 125408 (2005).
 - [13] S. Frank *et al.*, Science **280**, 1744 (1998).
 - [14] A. Urbina *et al.*, Phys. Rev. Lett. **90**, 106603 (2003).
 - [15] B. Stojetz *et al.*, Phys. Rev. Lett. **94**, 186802 (2005).
 - [16] F. Piéchon, Phys. Rev. Lett. **76**, 4372 (1996).
 - [17] R. Ketzmerick, *et al.*, Phys. Rev. Lett. **79**, 1959 (1997).
 - [18] J. C. Charlier and J. P. Michenaud, Phys. Rev. Lett. **70**, 1858 (1993). Ph. Lambin, V. Meunier, and A. Rubio Phys. Rev. B **62**, 5129-5135 (2000).
 - [19] Y. Last, J. Funct. Anal. **142**, 402 (1996); H. Schulz-Baldes and J. Bellissard, Rev. Math. Phys. **10**, 1 (1998).
 - [20] I. Guarneri, Europhys. Lett. **21**, 729 (1993); **10**, 95 (1989).
 - [21] R. Ketzmerick, G. Petschel, and T. Geisel, Phys. Rev. Lett. **69**, 695 (1992).
 - [22] T. Geisel, R. Ketzmerick, and G. Petschel, Phys. Rev. Lett. **66**, 1651 (1991).
 - [23] G. Paladin and A. Vulpiani, Phys. Rep. **156**, 147 (1987).
 - [24] A. I. Goldman and K. F. Kelton, Rev. Mod. Phys. **65**, 213 (1993).
 - [25] S. Roche, R. Saito, Phys. Rev. Lett. **87**, 246803 (2001).